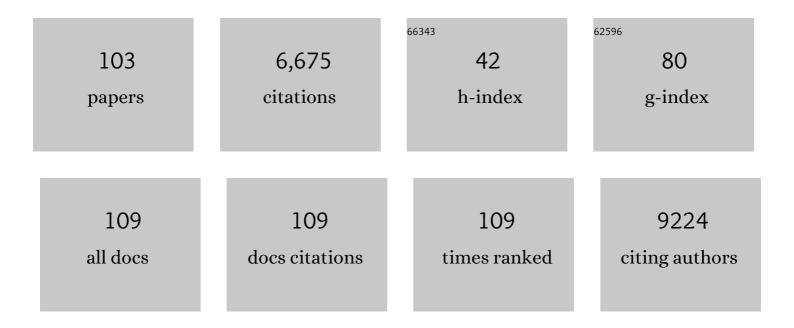
List of Publications by Year in descending order

Source: https://exaly.com/author-pdf/3531816/publications.pdf Version: 2024-02-01



ΗλΟ ΖΗΛΝΟ

#	Article	IF	CITATIONS
1	The Influence of Carboxyl Groups on the Photoluminescence of Mercaptocarboxylic Acid-Stabilized CdTe Nanoparticles. Journal of Physical Chemistry B, 2003, 107, 8-13.	2.6	581
2	CsPb <sub><i>x</i></sub> Mn <sub>1–<i>x</i></sub> Cl <sub>3</sub> Perovskite Quantum Dots with High Mn Substitution Ratio. ACS Nano, 2017, 11, 2239-2247.	14.6	496
3	Polymerâ€Passivated Inorganic Cesium Lead Mixedâ€Halide Perovskites for Stable and Efficient Solar Cells with High Openâ€Circuit Voltage over 1.3 V. Advanced Materials, 2018, 30, 1705393.	21.0	401
4	Assembly-Induced Enhancement of Cu Nanoclusters Luminescence with Mechanochromic Property. Journal of the American Chemical Society, 2015, 137, 12906-12913.	13.7	367
5	Inorganic CsPbI <sub>2</sub> Br Perovskite Solar Cells: The Progress and Perspective. Solar Rrl, 2019, 3, 1800239.	5.8	217
6	Alkylthiol-Enabled Se Powder Dissolution in Oleylamine at Room Temperature for the Phosphine-Free Synthesis of Copper-Based Quaternary Selenide Nanocrystals. Journal of the American Chemical Society, 2012, 134, 7207-7210.	13.7	213
7	Controllable Synthesis of Stable Urchin-like Gold Nanoparticles Using Hydroquinone to Tune the Reactivity of Gold Chloride. Journal of Physical Chemistry C, 2011, 115, 3630-3637.	3.1	196
8	Aurophilic Interactions in the Selfâ€Assembly of Gold Nanoclusters into Nanoribbons with Enhanced Luminescence. Angewandte Chemie - International Edition, 2019, 58, 8139-8144.	13.8	185
9	Contribution of Metal Defects in the Assembly Induced Emission of Cu Nanoclusters. Journal of the American Chemical Society, 2017, 139, 4318-4321.	13.7	152
10	Colloidal Synthesis of Ultrathin Monoclinic BiVO <sub>4</sub> Nanosheets for Z-Scheme Overall Water Splitting under Visible Light. ACS Catalysis, 2018, 8, 8649-8658.	11.2	151
11	Fe <sub>3</sub> O <sub>4</sub> @polydopamine Composite Theranostic Superparticles Employing Preassembled Fe <sub>3</sub> O <sub>4</sub> Nanoparticles as the Core. ACS Applied Materials & Interfaces, 2016, 8, 22942-22952.	8.0	135
12	Simple Synthesis of Highly Luminescent Water-Soluble CdTe Quantum Dots with Controllable Surface Functionality. Chemistry of Materials, 2011, 23, 4857-4862.	6.7	124
13	One-Step Preparation of Cesium Lead Halide CsPbX <sub>3</sub> (X = Cl, Br, and I) Perovskite Nanocrystals by Microwave Irradiation. ACS Applied Materials & Interfaces, 2017, 9, 42919-42927.	8.0	117
14	Photothermal-Activatable Fe <sub>3</sub> O <sub>4</sub> Superparticle Nanodrug Carriers with PD-L1 Immune Checkpoint Blockade for Anti-metastatic Cancer Immunotherapy. ACS Applied Materials & Interfaces, 2018, 10, 20342-20355.	8.0	112
15	Composite Photothermal Platform of Polypyrrole-Enveloped Fe <sub>3</sub> O <sub>4</sub> Nanoparticle Self-Assembled Superstructures. ACS Applied Materials & Interfaces, 2014, 6, 14552-14561.	8.0	108
16	Cu <sup>2+</sup> -Loaded Polydopamine Nanoparticles for Magnetic Resonance Imaging-Guided pH- and Near-Infrared-Light-Stimulated Thermochemotherapy. ACS Applied Materials & Interfaces, 2017, 9, 19706-19716.	8.0	103
17	Ultrathin BiOX (X = Cl, Br, I) Nanosheets with Exposed {001} Facets for Photocatalysis. ACS Applied Nano Materials, 2020, 3, 1981-1991.	5.0	100
18	Self-Assembly of Nanoclusters into Mono-, Few-, and Multilayered Sheets <i>via</i> Dipole-Induced Asymmetric van der Waals Attraction. ACS Nano, 2015, 9, 6315-6323.	14.6	98

#	Article	IF	CITATIONS
19	Hydroquinone-Assisted Synthesis of Branched Au–Ag Nanoparticles with Polydopamine Coating as Highly Efficient Photothermal Agents. ACS Applied Materials & Interfaces, 2015, 7, 11613-11623.	8.0	95
20	Self-Assembly Driven Aggregation-Induced Emission of Copper Nanoclusters: A Novel Technology for Lighting. ACS Applied Materials & Interfaces, 2018, 10, 12071-12080.	8.0	93
21	Engineering a red emission of copper nanocluster self-assembly architectures by employing aromatic thiols as capping ligands. Nanoscale, 2017, 9, 12618-12627.	5.6	87
22	Magnetic delivery of Fe <sub>3</sub> O <sub>4</sub> @polydopamine nanoparticle-loaded natural killer cells suggest a promising anticancer treatment. Biomaterials Science, 2018, 6, 2714-2725.	5.4	86
23	Polypyrrole-Coated Chainlike Gold Nanoparticle Architectures with the 808 nm Photothermal Transduction Efficiency up to 70%. ACS Applied Materials & Interfaces, 2014, 6, 5860-5868.	8.0	83
24	Quantum-Dot-Induced Self-Assembly of Cricoid Protein for Light Harvesting. ACS Nano, 2014, 8, 3743-3751.	14.6	83
25	Oxygen-Defective Ultrathin BiVO <sub>4</sub> Nanosheets for Enhanced Gas Sensing. ACS Applied Materials & Interfaces, 2019, 11, 23495-23502.	8.0	81
26	Colloidal Selfâ€Assembly of Catalytic Copper Nanoclusters into Ultrathin Ribbons. Angewandte Chemie - International Edition, 2014, 53, 12196-12200.	13.8	78
27	Energy Level Modification with Carbon Dot Interlayers Enables Efficient Perovskite Solar Cells and Quantum Dot Based Lightâ€Emitting Diodes. Advanced Functional Materials, 2020, 30, 1910530.	14.9	72
28	Enzyme-Triggered Defined Protein Nanoarrays: Efficient Light-Harvesting Systems to Mimic Chloroplasts. ACS Nano, 2017, 11, 938-945.	14.6	71
29	Facile Synthesis of Cu–In–S/ZnS Core/Shell Quantum Dots in 1-Dodecanethiol for Efficient Light-Emitting Diodes with an External Quantum Efficiency of 7.8%. Chemistry of Materials, 2018, 30, 8939-8947.	6.7	70
30	Engineering the Self-Assembly Induced Emission of Cu Nanoclusters by Au(I) Doping. ACS Applied Materials & Interfaces, 2017, 9, 24899-24907.	8.0	69
31	Polydopamine-coated Au-Ag nanoparticle-guided photothermal colorectal cancer therapy through multiple cell death pathways. Acta Biomaterialia, 2019, 83, 414-424.	8.3	68
32	Post-healing of defects: an alternative way for passivation of carbon-based mesoscopic perovskite solar cells <i>via</i> hydrophobic ligand coordination. Journal of Materials Chemistry A, 2018, 6, 2449-2455.	10.3	66
33	Engineering the Photoluminescence of CsPbX <sub>3</sub> (X = Cl, Br, and I) Perovskite Nanocrystals Across the Full Visible Spectra with the Interval of 1 nm. ACS Applied Materials & Interfaces, 2019, 11, 14256-14265.	8.0	66
34	Solution-Processed, Ultrathin Solar Cells from CdCl <sub>3</sub> <sup>–</sup> -Capped CdTe Nanocrystals: The Multiple Roles of CdCl <sub>3</sub> <sup>–</sup> Ligands. Journal of the American Chemical Society, 2016, 138, 7464-7467.	13.7	64
35	Cupreous Complex-Loaded Chitosan Nanoparticles for Photothermal Therapy and Chemotherapy of Oral Epithelial Carcinoma. ACS Applied Materials & Interfaces, 2015, 7, 20801-20812.	8.0	58
36	Surface Ligand Dynamics-Guided Preparation of Quantum Dots–Cellulose Composites for Light-Emitting Diodes. ACS Applied Materials & Interfaces, 2015, 7, 15830-15839.	8.0	57

#	Article	IF	CITATIONS
37	Iron oxide nanoparticles promote the migration of mesenchymal stem cells to injury sites. International Journal of Nanomedicine, 2019, Volume 14, 573-589.	6.7	54
38	Cu–Fe–Se Ternary Nanosheet-Based Drug Delivery Carrier for Multimodal Imaging and Combined Chemo/Photothermal Therapy of Cancer. ACS Applied Materials & Interfaces, 2018, 10, 43396-43404.	8.0	52
39	Aqueous-Processed Inorganic Thin-Film Solar Cells Based on CdSe <sub><i>x</i></sub> Te <sub>1–<i>x</i></sub> Nanocrystals: The Impact of Composition on Photovoltaic Performance. ACS Applied Materials & Interfaces, 2015, 7, 23223-23230.	8.0	48
40	Cu(II) doped polyaniline nanoshuttles for multimodal tumor diagnosis and therapy. Biomaterials, 2016, 104, 213-222.	11.4	48
41	Cu(II)-Doped Polydopamine-Coated Gold Nanorods for Tumor Theranostics. ACS Applied Materials & Interfaces, 2017, 9, 44293-44306.	8.0	45
42	In Situ Construction of Nanoscale CdTe CdS Bulk Heterojunctions for Inorganic Nanocrystal Solar Cells. Advanced Energy Materials, 2014, 4, 1400235.	19.5	44
43	Tumor Photothermal Therapy Employing Photothermal Inorganic Nanoparticles/Polymers Nanocomposites. Chinese Journal of Polymer Science (English Edition), 2019, 37, 115-128.	3.8	41
44	Hydrazine-Mediated Construction of Nanocrystal Self-Assembly Materials. ACS Nano, 2014, 8, 10569-10581.	14.6	40
45	Enhanced charge separation and photocatalytic hydrogen evolution in carbonized-polymer-dot-coupled lead halide perovskites. Materials Horizons, 2020, 7, 2719-2725.	12.2	38
46	Growth Kinetics of Aqueous CdTe Nanocrystals in the Presence of Simple Amines. Journal of Physical Chemistry C, 2010, 114, 6418-6425.	3.1	37
47	Synthesis of a Waterâ€Soluble Conjugated Polymer Based on Thiophene for an Aqueousâ€Processed Hybrid Photovoltaic and Photodetector Device. Advanced Materials, 2014, 26, 3655-3661.	21.0	35
48	Surfactant-Free Preparation of Au@Resveratrol Hollow Nanoparticles with Photothermal Performance and Antioxidant Activity. ACS Applied Materials & Interfaces, 2017, 9, 3376-3387.	8.0	35
49	<i>In vivo</i> migration of Fe <sub>3</sub> O <sub>4</sub> @polydopamine nanoparticle-labeled mesenchymal stem cells to burn injury sites and their therapeutic effects in a rat model. Biomaterials Science, 2019, 7, 2861-2872.	5.4	34
50	Surface Stabilization of Colloidal Perovskite Nanocrystals via Multi-amine Chelating Ligands. ACS Energy Letters, 2022, 7, 1963-1970.	17.4	34
51	Targeted multifunctional nanomaterials with MRI, chemotherapy and photothermal therapy for the diagnosis and treatment of bladder cancer. Biomaterials Science, 2020, 8, 342-352.	5.4	33
52	Phosphine-free synthesis of Ag–In–Se alloy nanocrystals with visible emissions. Nanoscale, 2015, 7, 18570-18578.	5.6	32
53	Targeting mitochondria with Au–Ag@Polydopamine nanoparticles for papillary thyroid cancer therapy. Biomaterials Science, 2019, 7, 1052-1063.	5.4	31
54	Efficient aqueous-processed hybrid solar cells from a polymer with a wide bandgap. Journal of Materials Chemistry A, 2015, 3, 10969-10975.	10.3	30

#	Article	IF	CITATIONS
55	High-Efficiency Aqueous-Processed Polymer/CdTe Nanocrystals Planar Heterojunction Solar Cells with Optimized Band Alignment and Reduced Interfacial Charge Recombination. ACS Applied Materials & Interfaces, 2017, 9, 31345-31351.	8.0	29
56	Tumor Microenvironment-Responsive Nanoshuttles with Sodium Citrate Modification for Hierarchical Targeting and Improved Tumor Theranostics. ACS Applied Materials & Interfaces, 2019, 11, 25730-25739.	8.0	29
57	Aurophilic Interactions in the Selfâ€Assembly of Gold Nanoclusters into Nanoribbons with Enhanced Luminescence. Angewandte Chemie, 2019, 131, 8223-8228.	2.0	29
58	Copper inter-nanoclusters distance-modulated chromism of self-assembly induced emission. Nanoscale, 2017, 9, 18845-18854.	5.6	29
59	"One-pot―synthesis and shape control of ZnSe semiconductor nanocrystals in liquid paraffin. Journal of Materials Chemistry, 2010, 20, 4451.	6.7	26
60	Fe(III)â€ <b>5</b> hikonin Supramolecular Nanomedicine for Combined Therapy of Tumor via Ferroptosis and Necroptosis. Advanced Healthcare Materials, 2022, 11, e2101926.	7.6	25
61	Nucleation of Aqueous Semiconductor Nanocrystals: A Neglected Factor for Determining the Photoluminescence. Journal of Physical Chemistry C, 2010, 114, 22487-22492.	3.1	24
62	Aqueousâ€Processed Polymer/Nanocrystals Hybrid Solar Cells: The Effects of Chlorine on the Synthesis of CdTe Nanocrystals, Crystal Growth, Defect Passivation, Photocarrier Dynamics, and Device Performance. Solar Rrl, 2017, 1, 1600020.	5.8	24
63	Aqueous-Processed Insulating Polymer/Nanocrystal Hybrid Solar Cells. ACS Applied Materials & Interfaces, 2016, 8, 7101-7110.	8.0	23
64	Paramagnetic CuS hollow nanoflowers for <i>T</i> <sub>2</sub> -FLAIR magnetic resonance imaging-guided thermochemotherapy of cancer. Biomaterials Science, 2019, 7, 409-418.	5.4	23
65	Alginate mediated functional aggregation of gold nanoclusters for systemic photothermal therapy and efficient renal clearance. Carbohydrate Polymers, 2020, 241, 116344.	10.2	23
66	Facile Synthesis of Cu <sub>2</sub> GeS <sub>3</sub> and Cu <sub>2</sub> MGeS <sub>4</sub> (M = Zn,) Tj ET Materials, 2016, 28, 9139-9149.	[Qq0 0 0 r 6.7	gBT /Overloc 22
67	Effect of Surface Trap States on Photocatalytic Activity of Semiconductor Quantum Dots. Journal of Physical Chemistry C, 2018, 122, 9312-9319.	3.1	22
68	Manipulating the growth of aqueous semiconductor nanocrystals through amine-promoted kinetic process. Physical Chemistry Chemical Physics, 2010, 12, 332-336.	2.8	21
69	Seedless synthesis of gold nanorods using resveratrol as a reductant. Nanotechnology, 2016, 27, 165601.	2.6	21
70	Electrophoretic deposition of fluorescent Cu and Au sheets for light-emitting diodes. Nanoscale, 2016, 8, 395-402.	5.6	21
71	Employing CdSe <sub><i>x</i></sub> Te <sub>1–<i>x</i></sub> Alloyed Quantum Dots to Avoid the Temperature-Dependent Emission Shift of Light-Emitting Diodes. Journal of Physical Chemistry C, 2017, 121, 5313-5323.	3.1	21
72	Microwave-Assisted Heating Method toward Multicolor Quantum Dot-Based Phosphors with Much Improved Luminescence. ACS Applied Materials & Interfaces, 2018, 10, 27160-27170.	8.0	21

#	Article	IF	CITATIONS
73	Phosphine-Free Synthesis of Metal Chalcogenide Quantum Dots by Directly Dissolving Chalcogen Dioxides in Alkylthiol as the Precursor. ACS Applied Materials & Interfaces, 2017, 9, 9840-9848.	8.0	20
74	Interstitial Nature of Mn <sup>2+</sup> Doping in 2D Perovskites. ACS Nano, 2021, 15, 20550-20561.	14.6	19
75	Seedless preparation of Au nanorods by hydroquinone assistant and red blood cell membrane camouflage. RSC Advances, 2018, 8, 21316-21325.	3.6	18
76	Deriving the colloidal synthesis of crystalline nanosheets to create self-assembly monolayers of nanoclusters. Advances in Colloid and Interface Science, 2014, 207, 347-360.	14.7	16
77	Constructing Postâ€Permeation Method to Fabricate Polymer/Nanocrystals Hybrid Solar Cells with PCE Exceeding 6%. Small, 2017, 13, 1603771.	10.0	16
78	Hollow Pd Nanospheres Conjugated with Ce6 To Simultaneously Realize Photodynamic and Photothermal Therapy. ACS Applied Bio Materials, 2018, 1, 1102-1108.	4.6	16
79	BiVO <sub>4</sub> @Bi <sub>2</sub> S <sub>3</sub> Heterojunction Nanorods with Enhanced Charge Separation Efficiency for Multimodal Imaging and Synergy Therapy of Tumor. ACS Applied Bio Materials, 2020, 3, 5080-5092.	4.6	16
80	NF-κB inhibition promotes apoptosis in androgen-independent prostate cancer cells by the photothermal effect <i>via</i> the lκBα/AR signaling pathway. Biomaterials Science, 2019, 7, 2559-2570.	5.4	15
81	Effect of Oleamine on Microwave-Assisted Synthesis of Cesium Lead Bromide Perovskite Nanocrystals. Langmuir, 2020, 36, 13663-13669.	3.5	14
82	<p>Magnetic Targeting of HU-MSCs in the Treatment of Glucocorticoid-Associated Osteonecrosis of the Femoral Head Through Akt/Bcl2/Bad/Caspase-3 Pathway</p> . International Journal of Nanomedicine, 2020, Volume 15, 3605-3620.	6.7	14
83	Advances in green colloidal synthesis of metal selenide and telluride quantum dots. Chinese Chemical Letters, 2019, 30, 277-284.	9.0	13
84	Homologous cancerous cell membrane modulated multifunctional nanoshuttles: Targeting specificity and improved tumor theranostics. Composites Communications, 2020, 20, 100342.	6.3	13
85	Ultrathin BiVO4 nanosheets sensing electrode for isopropanol sensor based on pyrochlore-Gd2Zr2O7 solid state electrolyte. Sensors and Actuators B: Chemical, 2020, 321, 128478.	7.8	13
86	A totally phosphine-free synthesis of metal telluride nanocrystals by employing alkylamides to replace alkylphosphines for preparing highly reactive tellurium precursors. Nanoscale, 2013, 5, 9593.	5.6	12
87	Efficacy of Fe <sub>3</sub> O <sub>4</sub> @polydopamine nanoparticle-labeled human umbilical cord Wharton's jelly-derived mesenchymal stem cells in the treatment of streptozotocin-induced diabetes in rats. Biomaterials Science, 2020, 8, 5362-5375.	5.4	10
88	Fe(III)-Doped Polyaminopyrrole Nanoparticle for Imaging-Guided Photothermal Therapy of Bladder Cancer. ACS Biomaterials Science and Engineering, 2022, 8, 502-511.	5.2	10
89	Multidrug resistant tumors-aimed theranostics on the basis of strong electrostatic attraction between resistant cells and nanomaterials. Biomaterials Science, 2019, 7, 4990-5001.	5.4	9
90	Copper Ion and Ruthenium Complex Codoped Polydopamine Nanoparticles for Magnetic Resonance/Photoacoustic Tomography Imaging-Guided Photodynamic/Photothermal Dual-Mode Therapy. ACS Applied Bio Materials, 2022, 5, 2365-2376.	4.6	9

#	Article	IF	CITATIONS
91	Cesium–Lead Bromide Perovskite Nanoribbons with Two-Unit-Cell Thickness and Large Lateral Dimension for Deep-Blue Light Emission. ACS Applied Nano Materials, 2020, 3, 4826-4836.	5.0	8
92	Z-Scheme heterostructures for glucose oxidase-sensitized radiocatalysis and starvation therapy of tumors. Nanoscale, 2022, 14, 2186-2198.	5.6	8
93	Analogous self-assembly and crystallization: a chloride-directed orientated self-assembly of Cu nanoclusters and subsequent growth of Cu <sub>2â^'x</sub> S nanocrystals. Nanoscale, 2017, 9, 10335-10343.	5.6	6
94	Asymmetric surface modification of yeast cells for living self-assembly. Chemical Communications, 2018, 54, 14112-14115.	4.1	6
95	Self-Assembly of Au Nanoclusters into Helical Ribbons by Manipulating the Flexibility of Capping Ligands. Langmuir, 2020, 36, 14614-14622.	3.5	6
96	Microwave-assisted synthesis of blue-emitting cesium bismuth bromine perovskite nanocrystals without polar solvent. Journal of Alloys and Compounds, 2021, 886, 161248.	5.5	6
97	Seed-mediated phase-selective growth of Cu <sub>2</sub> GeS <sub>3</sub> hollow nanoparticles with huge cavities. CrystEngComm, 2017, 19, 6736-6743.	2.6	5
98	Schwann Cell Migration through Magnetic Actuation Mediated by Fluorescent–Magnetic Bifunctional Fe <sub>3</sub> O <sub>4</sub> ·Rhodamine 6G@Polydopamine Superparticles. ACS Chemical Neuroscience, 2020, 11, 1359-1370.	3.5	5
99	Achieving full-color emission of Cu nanocluster self-assembly nanosheets by the virtue of halogen effects. Soft Matter, 2021, 17, 4550-4558.	2.7	5
100	Metal Nanoclusters/Polyvinyl Alcohol Composite Films as the Alternatives for Fabricating Remote-Type White Light-Emitting Diodes. Nanomaterials, 2022, 12, 204.	4.1	5
101	Electrostatic attraction driven and shuttle-like morphology assisted enhancement for tumor uptake. RSC Advances, 2017, 7, 56621-56628.	3.6	4
102	Chloride treatment for highly efficient aqueous-processed CdTe nanocrystal-based hybrid solar cells. Journal of Materials Chemistry C, 2018, 6, 11156-11161.	5.5	2
103	Long-lasting photoluminescence quantum yield of cesium lead halide perovskite-type quantum dots. Frontiers of Chemical Science and Engineering, 2021, 15, 187-197.	4.4	2